



HAL
open science

Fracture of M₂₃C₆ carbides / austenitic matrix interfaces in austenitic stainless steels

Y. Cui, M. Sauzay, P. Bonnaillie, Benoît Arnal

► To cite this version:

Y. Cui, M. Sauzay, P. Bonnaillie, Benoît Arnal. Fracture of M₂₃C₆ carbides / austenitic matrix interfaces in austenitic stainless steels. Creep 2015 - International Conference on Creep And Fracture Engineering Materials And Structure, May 2015, Toulouse, France. cea-02492572

HAL Id: cea-02492572

<https://hal-cea.archives-ouvertes.fr/cea-02492572>

Submitted on 27 Feb 2020

HAL is a multi-disciplinary open access archive for the deposit and dissemination of scientific research documents, whether they are published or not. The documents may come from teaching and research institutions in France or abroad, or from public or private research centers.

L'archive ouverte pluridisciplinaire **HAL**, est destinée au dépôt et à la diffusion de documents scientifiques de niveau recherche, publiés ou non, émanant des établissements d'enseignement et de recherche français ou étrangers, des laboratoires publics ou privés.

Fracture of $M_{23}C_6$ carbides / austenitic matrix interfaces in austenitic stainless steels

Y. CUI^{1,2}, M. SAUZAY¹, P. BONNAILLIE³, B. ARNAL⁴

¹. CEA, DEN, SRMA, LC2M, F-91191 Gif-sur-Yvette, France

². Université Paris 6 Pierre et Marie Curie, 75005, Paris, France

³. CEA, DEN, SRMP, F-91191 Gif-sur-Yvette, France

⁴. CEA, DEN, SRMA, LA2M, F-91191 Gif-sur-Yvette, France

Email: yiting.cui@cea.fr

The creep fracture of 316L(N) austenitic stainless steels has been studied both experimentally and theoretically for temperatures from 525°C up to 700°C and lifetimes up to nineteen years. Modeling and experimental study of long term creep damage in austenitic SSs [1] shows the followings:

1. For short term creep, failure is due to necking. Experimental lifetimes are bounded by the lower and upper bound predictions provided by a necking model and taking into account scatter in input parameters. This model leads to fair predictions of lifetimes up to a few thousand hours at very high temperature.
2. Based on FEG-SEM observations, the transition observed in the failure curves is due to intergranular cavitation. The Riedel modeling of cavity growth by vacancy diffusion along grain boundaries coupled with continuous nucleation is carried out. Lifetimes are predicted fairly well using this model for long term creep failure whatever the considered austenitic stainless steel (316L(N), 304H, 316H, 321H) and the applied temperature (525°C - 700°C). Taking into account low and high stress regimes of Norton-power law, the Riedel model allows us to predict the creep lifetimes up to 25 years which differ from experimental data by less than a factor 3.

It should be noted that no fitted parameter has been used as applying the Riedel model. But the cavity nucleation rate [2], \dot{N}_0 , should be deduced from cavity density measurements using FEG-SEM observations. This parameter is expressed in term of the number of cavities per unit grain boundary area and per unit time. This shows that the prediction of the cavity nucleation rate is the main remaining problem to be solved for getting physically based and reliable long term lifetime predictions. According to FEG-SEM observations, intergranular cavitation occurs mainly at $M_{23}C_6$ carbides / austenitic matrix interfaces (Fig. 1a). This is why the effect of the heterogeneity of the microstructure on grain boundary stress concentrations and cavity nucleation is simulated by the finite element method (Cast3M software). It aims to determine the distribution of grain boundary normal stress fields around precipitates depending on time and temperature. The features of the precipitates and the creep behavior of the austenitic matrix are both taking into account.

After FEG-SEM observations, for creep tests shorter than ten thousand hours, the majority of intergranular creep cavities are located at the interfaces of $M_{23}C_6$ carbides, along grain boundaries (Fig. 1a). Ten FEG-SEM micrographs carried out at a magnification of 1000X are analyzed using the image processing software, NOESIS-Visilog 7.2, to obtain the size distribution, the aspect ratio and orientation relative to the loading direction of the observed $M_{23}C_6$ precipitates. The mechanical properties of the considered carbides are found in literature. The creep behavior of the austenitic matrix is modelled using the Andrade law for the primary stage and the Norton law for the stationary stage. The parameters are adjusted using numerous

experimental creep curves. Many meshes including various configurations of $M_{23}C_6$ carbides located along grain boundaries embedded in the matrix are then built using the Cast3M FE software (Fig. 1b).

Different carbide parameters are considered in the finite element calculations, such as aspect ratio, spacing between carbides and geometry of the tips of the carbides. We are interested in the normal stress along $M_{23}C_6$ carbides / austenitic matrix interfaces. After a creep time of 4166h involving a strain of 8% at 600°C and 220MPa, the results show:

- Isolated carbide with an aspect ratio of 19 lead to an interface normal stress two times higher than an isolated circular carbide (Fig. 2a).
- Considering close neighbor precipitate increases the interface normal stress by a factor 1.8 with respect to an isolated carbide with an aspect ratio of 3 (Fig. 2b);

Considering all these microstructure details, the maximum normal stress along $M_{23}C_6$ carbides / austenitic matrix interfaces may reach 1.75GPa which is almost ten times higher than the remote stress. Taking into account the details of the carbide microstructure, it allows us to predict by continuum mechanics carbide interface normal stress of the same order of magnitude as the values computed by atomistic approaches. Finally, the interface fracture is simulated by using a cohesive zone modelling which parameters are computed by DFT. The predicted cavity nucleation rate, which is the only material parameter missing from the theoretical point of view, will be compared to our measured values at different temperatures and applied stresses.

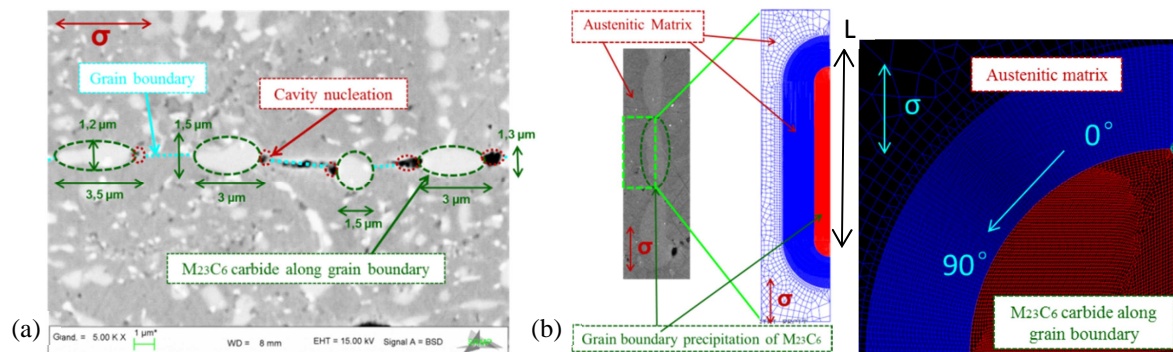


Figure 1: (a) FEG-SEM image, creep test, longitudinal section, 700°C, 100MPa, 2226h. (b) Mesh of a $M_{23}C_6$ carbide embedded in an austenitic matrix and mesh refinement along the carbide interface. The loading direction is vertical. The carbide length is expressed as L.

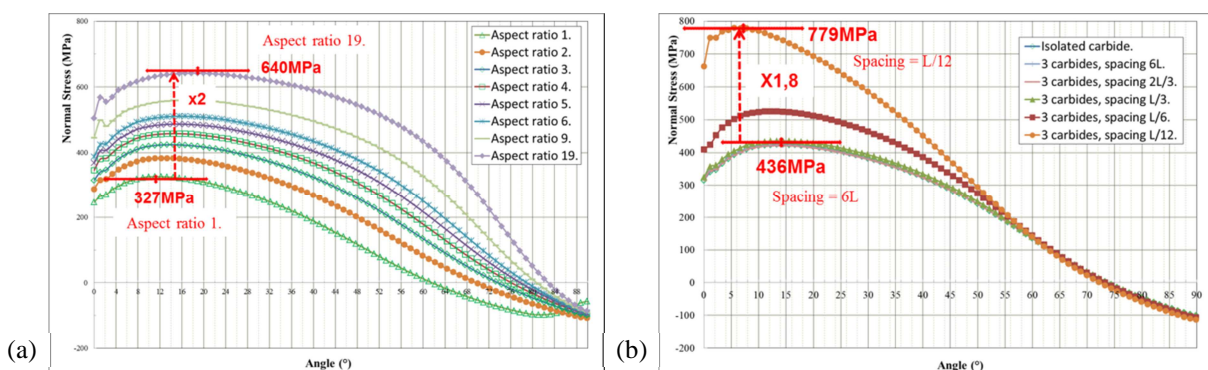


Figure 2: Distribution of normal stress along $M_{23}C_6$ carbides / austenitic matrix interfaces after a creep time of 4166h involving a strain of 8% at 600°C and 220MPa, (a) effect of the carbide aspect ratio, (b) effect of the inter-carbide spacing for an aspect ratio of 3.

References

- [1] Y. T. Cui, M. Sauzay, et al., *Procedia Mater. Sci.*, vol. 3, pp. 122–128, 2014.
- [2] B. F. Dyson, *Scr. Metall.*, vol. 17, no. 1, pp. 31–37, Jan. 1983.